

RESEARCH

Open Access



Influence of functionalized S–SBR on silica–filled rubber compound properties

Chigusa Yamada^{1,2*}, Atsushi Yasumoto², Tadashi Matsushita² and Anke Blume¹

Abstract

Styrene–butadiene–Rubber, SBR, is most often used in tread compounds in order to improve the Rolling Resistance (RR). The functionalized SBRs are used to increase the polymer–filler interaction in the compound to improve RR. In this study, the effect of different types of functional groups in SBR was investigated. Several types of functionalized S–SBRs were synthesized by anionic polymerization: (i) SBR with an amine group at one end of the polymer chain, (ii) SBR with an alkoxy silane group at one end (iii) SBR with an amine group at one end and an alkoxy silane group at the other end of the polymer chain. A model reaction of silanization was conducted in a solvent to estimate how the amine functional group affects the silanization. Silica filled compounds were prepared with these SBR types. Payne effect and bound rubber measurement were done. The model silanization reaction of TESPT (Bis(triethoxysilylpropyl) tetrasulfide) with silica in the presence of amine shows that a higher amount of ethanol (EtOH) is released from TESPT compared to the amine free system. This result indicates that the silanization reaction can be accelerated by the presence of an amine functional group at the SBR polymer chain used in silica–filled compounds. The amine functionalized SBR and the alkoxy silane functionalized SBR show less Payne effect of the compounds which indicates that both functional groups can decrease the filler–filler interaction. More chemical bound rubber was obtained in branched SBRs compared to the corresponding linear SBRs. A branched polymer chain has a higher molecular weight compared to the linear type. Therefore, when one branched polymer chain reacts with silica or creates a silica–silane–polymer bond, more bound rubber can be obtained for the branched than for the linear type. The compound of the SBR with the alkoxy–silane functional group shows lower $\tan \delta$ compared to the non–functionalized SBR and the amine functionalized SBR compounds. The influence of the type of functionalization of the SBR on $\tan \delta$ at 70 °C was more significant in branched SBRs than in linear SBRs, due to the before–mentioned effect of the functional group on silanization and bound rubber.

Keywords: SBR, Functionalization, Rolling resistance, Silica

Background

In terms of conservation of energy and natural resources, the fuel efficiency of tires comes more and more into focus over the last years. As the contribution of the RR of tires to the fuel consumption is generally known to be around 10%, which is relatively high, it is a significant issue to reduce the RR of tires [1]. One of the major

developments in the tire industry of the last decennia is the introduction of silica to replace carbon black for a significant reduction of the rolling resistance and improvement of the wet grip. However, due to its high degree of filler–filler interaction, it is difficult to disperse silica within the rubber compounds. In 1992, a silica–filled green tire tread compound was invented by Michelin. Since then, silica–filled compounds play a major role in the tire industry [2]. An alternative promising approach is the functionalization of the elastomer matrix for improving the dispersibility of silica and for introducing a direct silica–polymer interaction.

*Correspondence: c.yamada@utwente.nl

¹ Elastomer Technology and Engineering, University of Twente, Enschede (NL), P.O. Box 217, 7500AE Enschede, the Netherlands
Full list of author information is available at the end of the article

Styrene–butadiene–Rubber, SBR, is most often used in tread compounds in order to improve the RR. There are two types of SBRs, one is Emulsion SBR (E–SBR) and another one is Solution SBR (S–SBR). A great advantage of S–SBR is that a functional moiety can be easily introduced in the SBR, which enables stronger filler–polymer interaction resulting in better silica dispersion. In 1980's, a functionalization technology using a tin agent was already reported by Edwards [3]. There are four major methods to functionalize SBR [3–7]. Firstly, functionalized SBR can be prepared by terminating the anionic polymerization with a functional agent. Secondly, an initiator with functional moiety can be used to introduce the functional group at the polymerization initiating terminal side. Thirdly, the functional group can be introduced in the polymer main chain by adding a third monomer with a functional moiety during the polymerization [8]. The last option is to use a functional agent which can react with the vinyl groups of SBR, resulting in the functionalization of the main chain.

Many studies of different functionalized SBRs were carried out. The influence of introducing γ -chloropropyl trimethoxy silane (CPTMO) on SBR chain–ends was investigated and the dispersion of silica and some related mechanical properties were studied [9]. Hassanabadi et al. investigated the influence of different functional groups in SBR on the performance of silica–filled compounds [10]. An SBR with a 3-(aminopropyl)triethoxysilane group (APTES) showed the best wear resistance and tear resistance. However, the influence of the macro-structure of polymer (e.g., the number of arms) was not discussed.

The pronounced decrease of the storage modulus with increasing strain amplitude is known as “Payne effect” and used as an indicator for the filler–filler

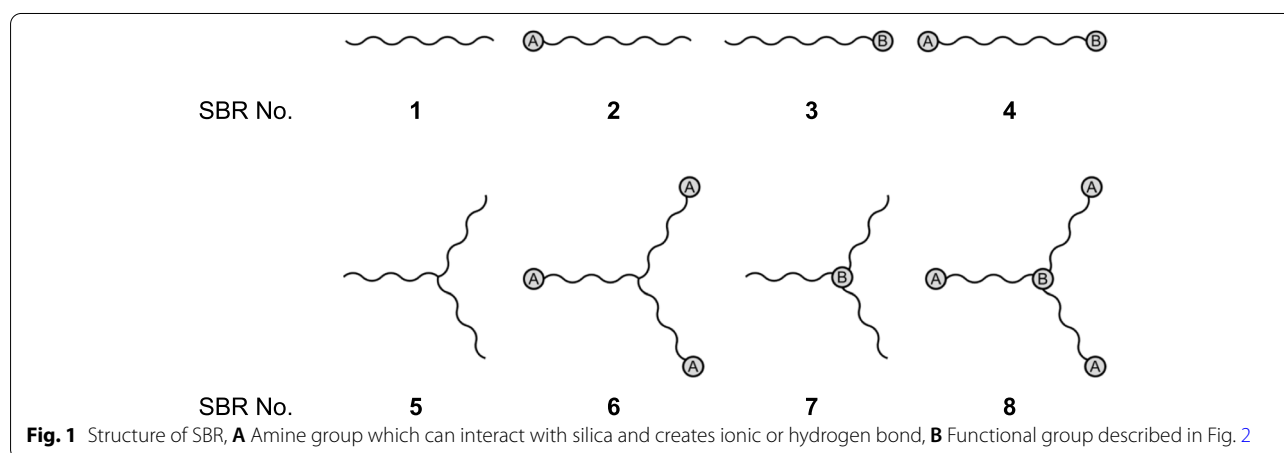
interaction. The filler–filler interaction affects the material characteristics as described by Payne [11]. Furthermore, small–angle scattering (SAXS) is a unique tool to investigate the morphological structure of fillers in rubber matrices. Koga et al. investigated the hierarchical structures of carbon black with small–angle scattering using a modified approach to extract not only the particle sizes but also the shapes of the structure elements [12]. Mihara et al. utilized this method for silica compounds and investigated the influence of the silica particle size on the mechanical properties [13, 14].

In this study, the influence of different types of functional groups in SBR with different macro-structure on the in–rubber properties of silica filled compounds was investigated. The experimental data were analyzed by means of Payne effect, SAXS, bound rubber, and $\tan \delta$ measurements. The model reaction in the solvent was conducted to investigate the effect of the different functional groups on the silanization reaction.

Methods

Materials

Eight types of SBRs are used in this study (Fig. 1 and Table 1). Three functionalization technologies were applied to these polymers. Functionalized A type has an amine group at one chain end. Functionalized B polymer has an alkoxy silane and amine group at one chain end. Both–ends functionalized SBR has both of these functional groups at each end of the polymer chain. A non–functionalized type is used as a reference. For each type of SBRs, a branched–structured SBR was also prepared. The functional group B in the branched types is slightly more active in comparison with that one inside the linear types.



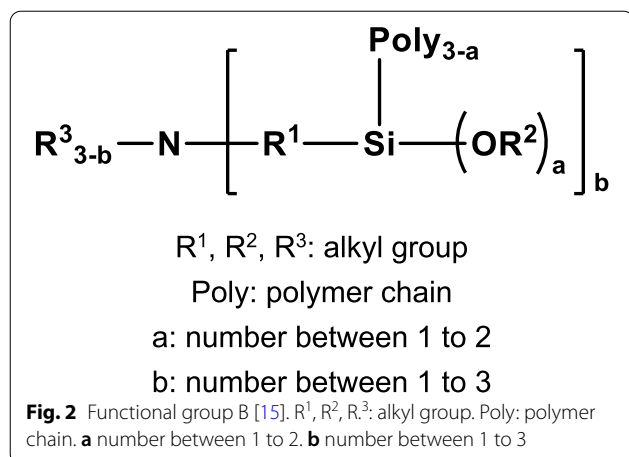


Table 2 Rubber compounds composition (phr)

Ingredient	Product name	Producer	Phr
SBR	Varying types		80
BR	UBEPOL BR [®] 150	UBE	20
Silica	ULTRASIL [®] 7000 GR	Evonik	75
TESPT	Si69 [®]	Evonik	5.6
TDAE Oil	VIVATEC 500	Hansen & Rosenthal	36
Zinc Oxide		Merck	2.5
Stearic Acid		Merck	2
6PPD	VULKANOX 4020/LG	Lanxess	2
Wax	Sasolwax 6403	Sasol Wax GmbH	1.5
Sulfur		J. T Baker	2.2
CBS	Santocure CBS	Flexsys	1.7
DPG	Perkacit DPG	Flexsys	2

Formulation and mixing

A typical green tire tread composition was chosen for the compounds which is shown in Table 2.

The compounds were prepared in an internal batch mixer (Brabender Plasticorder 350S (390 cc)). The mixing was started at 90 °C and 50 rpm. The compounds were mixed in this mixer in the first stage. The vulcanization system was added to the compound in a second mixing stage, which was done on a two-roll mill where the compounds were finally formed into sheets (Table 3).

Green compound properties

The Payne effect of the 1st masterbatch was measured by a Rubber Process Analyzer, RPA 2000 of Alpha Technologies, the test condition was 100 °C, 0.56% – 400%, 1 Hz.

SAXS measurement

SAXS was measured by a Rigaku NANOPIX (wavelength: 0.154 nm, exposure time: 900 s, distance from the sample to the detector: 1312 mm). X-rays are transmitted through the sample, and the scattered X-rays at that time are captured by a two-dimensional detector (Hypix-6000, Rigaku) (Fig. 3).

Table 3 Mixing procedure

1st stage	Internal mixer
Time	
0:00	Polymers
1:20	1/2 silica, 1/2 TESPT, Oil
2:50	1/2 silica, 1/2 TESPT, Stearic acid, Zinc oxide
3:10	Mix (Control rotor speed up to 140 °C)
4:10	Ram up, sweep, ram down
6:40	Dump out
2nd stage	Two-roll mill
0:00	1st masterbatch
2:00	Sulfur, CBS, DPG
7:00	Milling

The obtained two-dimensional data is converted to one-dimensional scattering profile, I(q) by circular average. $q = 4\pi\sin\theta/\lambda$ is the magnitude of the scattering vector where λ , 2θ are the wavelength of the incident beam and the scattering angle, respectively.

Table 1 Properties of SBRs

No	Type	Styrene (%)	Vinyl (%)	ML ₁₊₄ 100 °C	Number of arms	M _w (kg/mol)	M _w /M _n
1	Linear	27	43	45	1	277	1.1
2	Linear	26	43	45	1	262	1.1
3	Linear	27	43	47	1	253	1.2
4	Linear	27	43	42	1	241	1.2
5	Star	26	42	66	3–4	520	1.2
6	Star	26	42	66	3–4	492	1.2
7	Star	26	42	66	3–4	472	1.2
8	Star	26	41	64	3–4	453	1.2

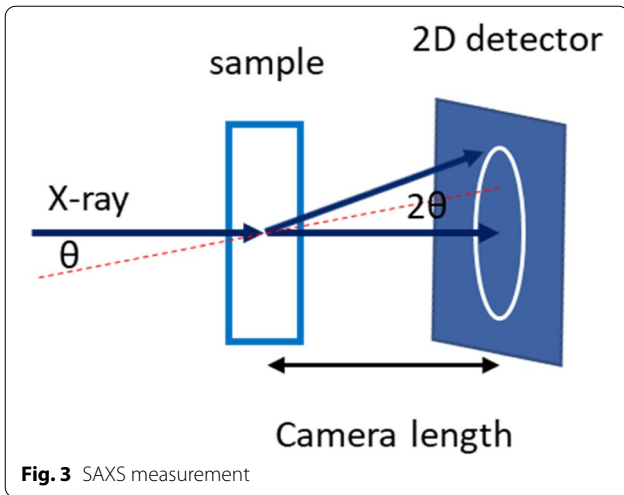


Fig. 3 SAXS measurement

It is reported that carbon black generates the hierarchical structure in rubber compounds (Fig. 4) [12]. Based on this structure, the theoretical Eq. (1) was proposed.

$$\begin{aligned}
 I(q) = & C \exp(-q^2 R_{ss}^2/3) q^{-D_m} \\
 & + D \exp(-q^2 R_{ss}^2/3) \\
 & + E [\text{erf}(q R_{ss}/6)]^{3(2d-D_s)} q^{-(2d-D_s)}
 \end{aligned}
 \tag{1}$$

C, D, E: coefficient

D_m: mass fractal dimension of agglomerates at level 2

D_s: the surface fractal dimension of primary particles

d: the Euclidean dimension of the space (= 3)

R_{ss}: radius of gyration of agglomerate at level 1

erf(*x*): the error function

This concept was used in the present paper to evaluate the silica dispersion. At first, the experimental *I*(*q*) was described by Eq. (1). Here, *D_m* was set to be constant at 2.3, using the same value for silica as it is described for carbon black in the reference paper [12]. However,

Eq. (1) did not represent the experimental SAXS profiles in the current study. This is because the SAXS profile shows a shoulder originating from the form factor of primary silica particles, which is absent in SAXS profiles shown in [10].

To solve this issue, another model was applied to estimate the size of silica agglomerates in the compound. The main modification to Eq. (1) is that a term for scattering from primary silica particles, *I_{silica}*(*q*) was added. In this model, *I_{silica}*(*q*) is expressed by the form factor of isolated spheric particles as following Eq. (2) and (3)

$$I_{silica}(q) = \Delta\rho_{e,silica}^2 \int_0^\infty P_{silica}(r) \left[\frac{4\pi r^3}{3} \Phi(qr) \right]^2 dr
 \tag{2}$$

$$\Phi(qr) = \frac{3}{(qr)^3} [\sin(qr) - qr \cos(qr)]
 \tag{3}$$

$\Delta\rho_{e,silica}$ is the difference of electron density between primary silica particles and polymer matrix. Particle volume distribution of radius, *p_{silica}*(*r*) is assumed to follow the Schulz–Zimm distribution [11]. The particle number distribution of radius, *P_{silica}*(*r*) is calculated from *p_{silica}*(*r*) as shown in Eq. (4), (5) and (6)

$$p_{silica}(r) = \frac{M^M}{\Gamma(M)r_{silica}^M} r^{M-1} \exp\left(-\frac{M}{r_{silica}}r\right)
 \tag{4}$$

$$M = (\sigma/r_{silica})^{-0.5}
 \tag{5}$$

$$P_{silica}(r) = \frac{p(r)/V(r)}{\int p(r)/V(r)dr}
 \tag{6}$$

Here, *r_{silica}* and σ is the average radius and standard deviation of radius, respectively. *V*(*r*) = 4π*r*³/3 is the particle volume. Furthermore, it is considered that the radius distribution of the agglomerates and modified the second term in Eq. (1) to *I_{2nd}*(*q*) as following (Eq. (7)).

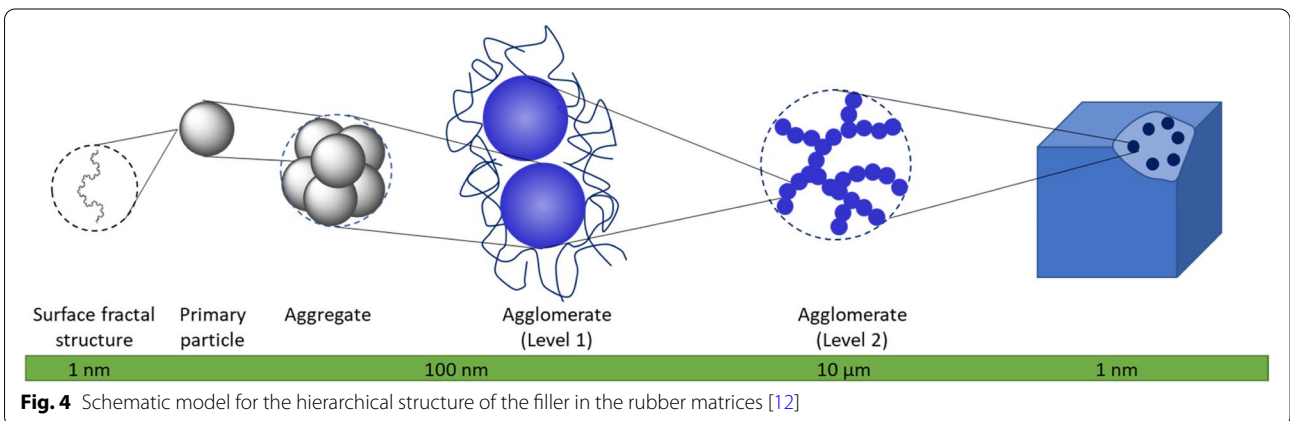


Fig. 4 Schematic model for the hierarchical structure of the filler in the rubber matrices [12]

$$I_{2nd}(q) = \Delta\rho_{e,2nd}^2 \int_0^\infty P_{2nd}(r) \left[\frac{4\pi r^3}{3} \Phi(qr) \right]^2 dr \quad (7)$$

$\Delta\rho_{e,2nd}$ is the difference between average electron density of the agglomerates and that of the polymer matrix. Here, it is assumed that the shape of the agglomerates is spherical and the volume distribution of radius of the agglomerates $p_{2nd}(r)$ follows the Schultz–Zimm distribution [11]. The number distribution of radius of the agglomerates, $P_{2nd}(r)$, is calculated from $p_{2nd}(r)$ as already shown in Eq. (4). Eventually, the following scattering function to describe the SAXS profiles is proposed.

$$I(q) = n[A \exp\{-q^2(\sqrt{3}r_{2nd})^2/3\} q^{-Dm} + I_{2nd}(q) + n_s I_{silica}(q) + B\{\text{erf}(qr_{silica}/\sqrt{6})\}^{3(6-Ds)} q^{-(6-Ds)}] \quad (8)$$

A, B: coefficient.

n: Number density of secondary aggregates. “Secondary aggregates” means that the cluster consists of several primary particles, equivalent to “agglomerates at level 1” presented in [10].

n_s : The number of primary particles in secondary aggregates.

r_{2nd} , r_{silica} : Average radius of secondary aggregates and primary silica particles, respectively.

By the fitting analysis based on Eq. (8), the average size of second aggregates of silica, r_{2nd} can be obtained.

Bound rubber measurement

Bound rubber measurements were done for all green compounds. Physical bound rubber and chemical bound rubber were measured in the following way [16]: 0.2 g of each green compound was immersed in toluene at room temperature for 7 days. After that, the sample was removed from the toluene and dried at 70 °C in the vacuum oven for 24 h. The bound rubber content was calculated according to Eq. (9).

$$\text{Bound rubber content (\%)} = \frac{W_{fg} - W \frac{m_f}{m_f + m_p}}{W \frac{m_p}{m_f + m_p}} \times 100 \quad (9)$$

where W_{fg} is the weight of the specimen after dried, W is the original weight of the specimen, and m_f and m_p are the weights of filler and polymer in the compound, respectively.

The same procedure was done in ammonia atmosphere to cleave the physical linkages between rubber and silica, so that the chemically bound rubber can be determined. The amount of physical bound rubber was calculated according to Eq. (10).

$$m_{\text{physical bound rubber}} = m_{\text{bound rubber without ammonia treatment}} - m_{\text{chemical bound rubber}} \quad (10)$$

$m_{\text{bound rubber without ammonia treatment}}$: percentage of bound rubber measured without ammonia treatment.

$m_{\text{chemical bound rubber}}$: percentage of bound rubber measured with ammonia treatment.

Curing

The samples were vulcanized in a Wickert press WLP 1600 at 100 bar and 160 °C, according to their $t_{90} + 5$ min optimum vulcanization time, as determined by an RPA 2000 of Alpha Technologies, following the procedure described in ISO 3417.

Tensile properties

Tensile properties are measured following the procedure described in ISO 37.

Viscoelastic properties of vulcanized compound

Tan δ at 70 °C, an indicator of rolling resistance was measured by RPA 2000 of Alpha Technologies. The samples were cured in this device at 100 bar and 160 °C, according to their $t_{90} + 5$ min optimum vulcanization time, then the temperature was decreased to 70 °C and kept for 10 min. After that, the measurement was performed with at 70 °C, at 0.56% – 400% and at 10 Hz. Tan δ measured at 70 °C at 6% strain and at 10 Hz was used as the indicator of rolling resistance.

Model reaction

The rate of reaction between TESPT and silica in the presence of amine as the functional group was measured in a model system. 0.2 g of TESPT, 2 g of silica, 2 ml of n-decane and 0.001 g of amine A were weighed in the reaction ampoule. The ampoules were dipped into an oil bath at a specified temperature for different reaction times. 2 ml of diethyleneglycol–monobutylether was added after the reaction to remove all physical–bonded silane at the silica surface and to desorb the absorbed ethanol [17]. The reaction mixture was filtered by using a 45 mm porous filter. The amount of ethanol was measured by gas chromatography to estimate the degree of silanization.

Results

Model reaction

The acceleration of the silanization depends on the rate of hydrolysis of the alkoxy silanes [18]. It is known

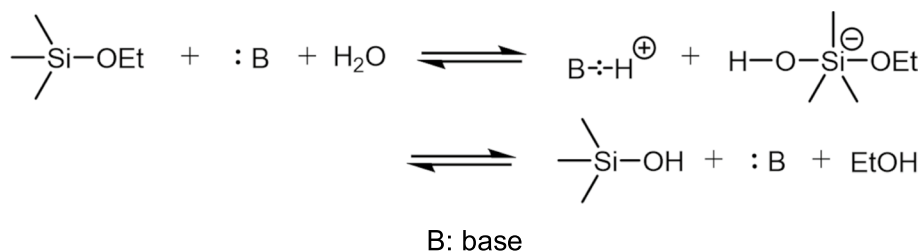


Fig. 5 Hydrolysis reaction of silane coupling agent [18]. B: base

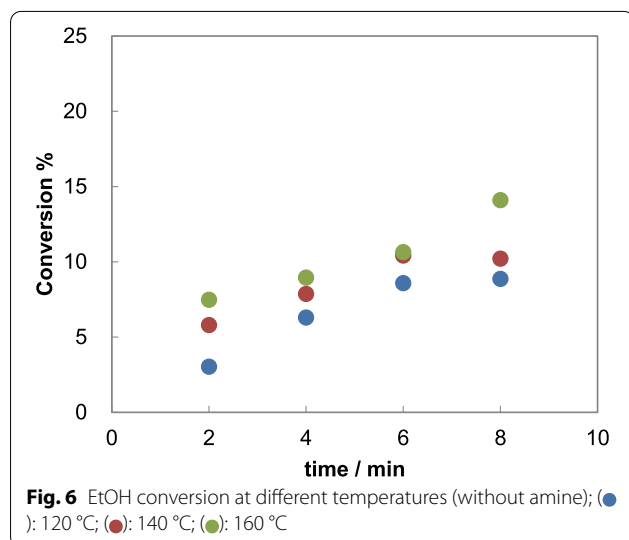


Fig. 6 EtOH conversion at different temperatures (without amine); (●): 120 °C; (●): 140 °C; (●): 160 °C

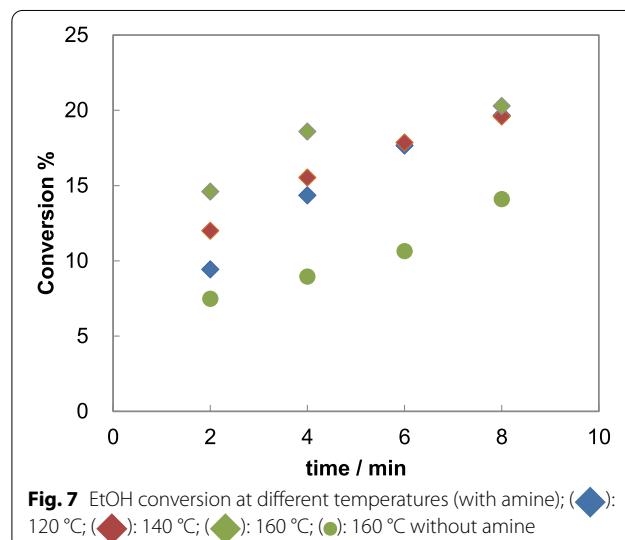


Fig. 7 EtOH conversion at different temperatures (with amine); (◆): 120 °C; (◆): 140 °C; (◆): 160 °C; (●): 160 °C without amine

that the hydrolysis of silane is accelerated by the presence of a base, such as amine (Fig. 5) [19]. During the reaction, EtOH is released from TESPT. The amount of EtOH was measured to estimate the degree of silanization. The conversion of EtOH is calculated with 100% representing the amount of all EtOH which can be theoretically released from TESPT.

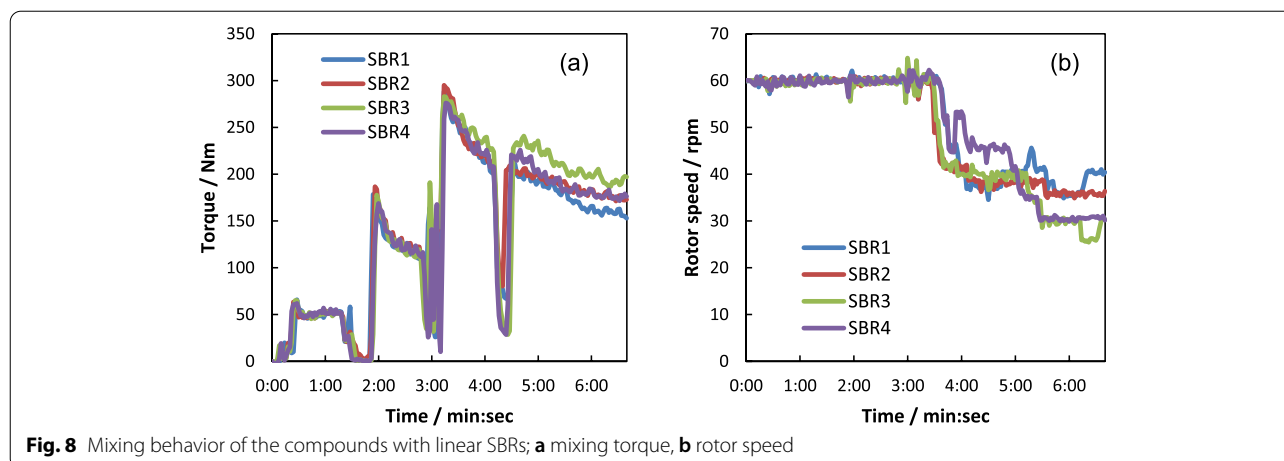
The EtOH conversion at different temperatures of an amine free system is shown in Fig. 6. The conversion increased significantly with increasing temperature. It indicates that the silanization reaction was accelerated at higher temperature. This fits to previous findings in the literature [20].

The same reaction was conducted in the presence of amine which has the same chemical structure as the functional group in the modified SBR. As shown in Fig. 7, the amount of EtOH increases to a higher degree in the presence of amine compared to the result without amine. This shows clearly that amine can accelerate the silanization reaction. It can be therefore expected that the amine-group in the modified SBR can also accelerate the silanization reaction in the compound.

Mixing behavior

Mixing torque and rotor speed are depicted in Figs. 7 and 8. The rotor speed was adjusted to keep 140 °C temperature after all ingredients added to the mixer. The mixing torque can be influenced by the rotor speed as well as by the incorporation of silica, the viscosity of the polymer and the polymer–filler interactions.

The mixing torque of SBR 2, SBR 3 and SBR 4 compounds after all ingredients added at 3 min is higher compared that of SBR 1, because there is a higher polymer–filler interaction due to the functional groups in SBR. The slightly higher torque is observed in the mixing curve of SBR 2 compound compared to SBR 1. The rotor speed is slightly lower. These behaviors indicate that there is a higher polymer–filler interaction due to the presence of the functional group A in SBR 2. Due to the high shear during the mixing, the rotor speed was kept lower than that of SBR 1 to keep the same temperature of silanization for all compounds. The SBR 3 shows an even higher torque and lower rotor speed. This implies that the functional group B in SBR 3 creates higher polymer–filler interaction compared to the functional group A in SBR 2. The torque of SBR 4 is close to that of SBR 2,



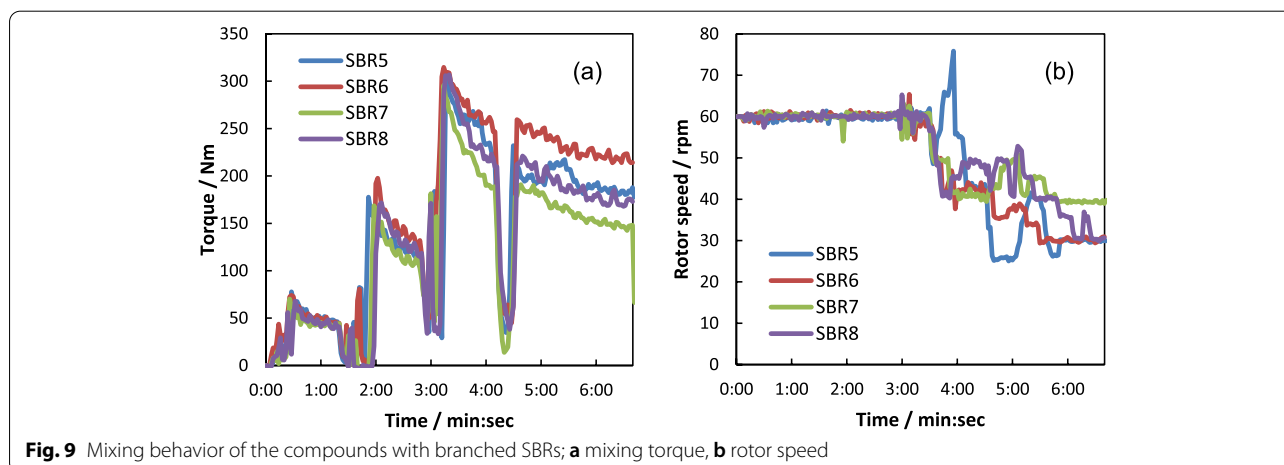
however, the rotor speed is comparable with that of SBR 3. As SBR 4 is expected to show the highest polymer–filler interaction because it has both functional groups A and B, the silica filler incorporation might be fast in this compound which leads to less shear forces compared to SBR 3. Therefore, a slightly lower torque is observed in SBR 4 compared to SBR 3.

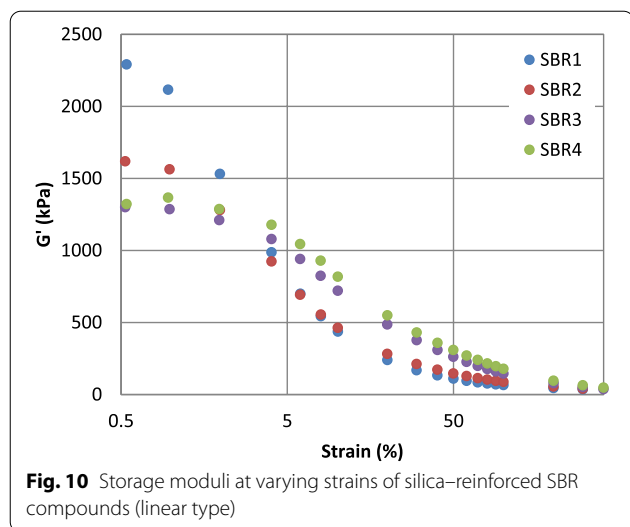
For the compounds with branched SBRs, the difference of their mixing behaviors is more significant (Fig. 9). SBR 6 shows the highest mixing torque and the lowest rotor speed compared to all other SBR compounds. This tendency is not observed in the linear type SBR (SBR 2). The number of the functional group A in SBR 6 is higher compared to the corresponding linear type (SBR 2), therefore, there is a higher polymer–filler interaction in the SBR 6 compound which causes a higher viscosity resulting in a higher torque. SBR 7 shows the lowest mixing torque which is not seen in the linear type (SBR 3). This indicates a fast silica incorporation in the SBR 7 compound. The mixing torque of SBR 8 is slightly higher

than that of SBR 7 which indicates a higher polymer–filler interaction, because again the number of the functional group A is higher in SBR 8. Therefore, the mixing torque of SBR 7 is the lowest of all investigated branched type SBR compounds.

Payne effect of the green compounds

The Payne effect in filled rubber is the phenomenon of a strain dependent dynamic modulus which decreases with increasing strain [21]. The Payne effect value (the gap of the storage modulus at lower strain and that of higher strain) is known as an indicator for the degree of filler–filler interactions of the filled rubber compounds and it correlates the micro–dispersion [22, 23]. Especially, silica filled compounds show a high Payne effect, because the hydroxy groups at the silica surface create hydrogen bonds between silica particles. The strain sweep data of the compounds containing the linear polymers are exhibited in Fig. 10. It is evident that the storage modulus at 0.56% strain decreases for the functionalized SBR 2, 3





and 4 compared to the unmodified reference SBR. The compound of both-ends functionalized SBR 4 shows higher storage moduli over the whole strain range compared to functionalized SBR 3, which indicates a stronger filler-polymer interaction by both functionalizations. With both-ends functionalization, this SBR can create a network structure in the compounds, because both-ends can interact or react with the silanol groups at the silica surface. There is a plateau part at the lower strain region of functionalized SBR 3 and 4. This also indicates that the filler clusters cannot be easily broken by the deformation due to the strong filler-polymer interaction. The indicator of the filler-filler interaction ($\Delta G'$, the gap of the storage moduli at 0.56% strain and that of 100% strain) is summarized in Table 4. The value of $\Delta G'$ is significantly reduced by using functionalized SBR.

The storage modulus at high strain (100%) is an indicator for crosslinks in the rubber matrix, because the filler-filler network is already broken down at this strain. These cross-links consist of the sulfur-crosslinking of the polymer chains, the silica-silane-polymer coupling and the functionalized polymer-silica coupling. As shown in Table 4, the highest storage modulus at 100% was obtained in the compound of alkoxy silane functionalized SBR 4. Comparison with non-functionalized SBR 1, amine

functionalized SBR 2 shows slightly higher storage modulus. This is due to the stronger filler-polymer interaction in the rubber matrix.

The strain sweep data of the compounds with the branched SBRs is depicted in Fig. 11. The same tendency was obtained as for the linear SBRs. The functionalized SBRs 6, 7 and 8 show a lower storage modulus at 0.56% compared to the non-functionalized branched SBR 5. This tendency is seen in $\Delta G'$ as depicted in Table 4. The storage modulus at high strain (100%) of SBR 6, which has an amine-functionalization at the polymer chain ends, is clearly higher than that of SBR 5, which was not observed in the comparison of the linear type SBRs. The amount of amine in one polymer molecule is higher in the branched SBR than that in the linear SBR, therefore, a higher filler-polymer interaction is obtained in the branched SBR resulting in a higher storage modulus at high strain.

SAXS

R_{ss} calculated from Eq. 1 is shown in Fig. 12. The R_{ss} value of the compound with functionalized SBR 3, 4, 7 and 8, alkoxy silane functionalized SBRs, is slightly lower compared to all other compounds. The tendency is not the same as the result from the Payne effect measurements. This might be based on the fact

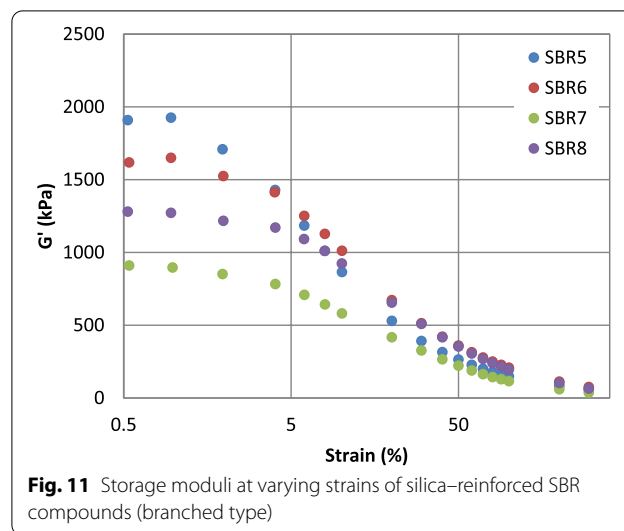
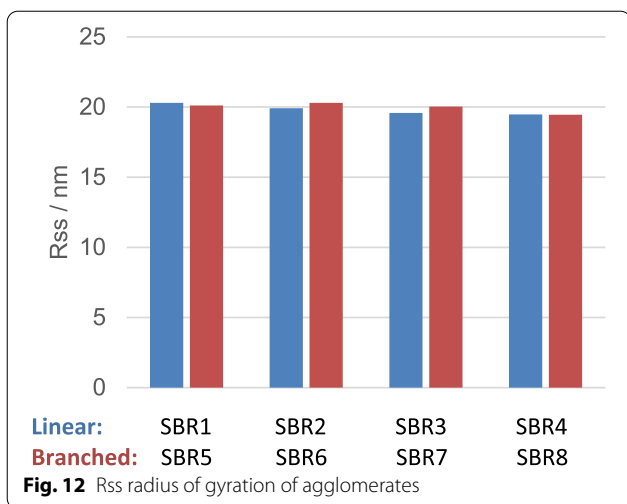


Table 4 Storage moduli at low strain and high strain

	unit	SBR1	SBR2	SBR3	SBR4	SBR5	SBR6	SBR7	SBR8
G' at 0.56% strain	kPa	2291	1619	1301	1322	1909	1618	910	1281
G' at 100% strain	kPa	66	88	145	178	148	208	115	196
$\Delta G'$	kPa	2226	1531	1155	1144	1760	1411	795	1085



that the Payne effect does not correlate with the silica size which is detected by SAXS measurements or the related degree of micro-dispersion in the compounds. This SAXS measurement detects only the silica cluster with the size between a few nm to a few hundred nm. This is just a part of the micro-dispersion range, considered in the literature to be smaller than 2 μm [24]. However, the difference of R_{ss} between each compound is very small.

Focusing of the SAXS profile, (Fig. 13), there is a difference between both profiles between $q=0.04$ to 0.3 which are derived from the silica cluster (the range marked with an arrow).

reported in the past [14, 25], this difference indicates the different silica sizes. This result indicates that the modification is necessary for Eq. 1.

In order to investigate the SAXS result in detail, the average silica particle size from the calculation of Eq. 2 is depicted in Fig. 14. Considering the measurement error of $\pm 3\%$, the difference between each compound is clearer compared to the results in Fig. 12. The average silica particle size of the compound with the non-functionalized SBR is the same as that of the compound with amine-functionalized SBR in both linear and branched types. This trend is different to that one observed in the Payne effect. The Payne effect of non-functionalized SBR is higher than that of the amine-functionalized SBR. On the one hand, the Payne effect is used as an indicator of micro-dispersion where the filler size is smaller than 2 μm [23, 26], on the other hand, the resolution limit of SAXS contains few nm to hundreds nm [27]. As the exact particle size of silica which influences the Payne effect is not clear, it can be concluded that these two measurements detect slightly different size ranges, resulting in different trends. The average particle size of silica inside the alkoxy silane functionalized SBR compound is clearly smaller than that inside the non-functionalized SBR compound. This is true for both SBR types, the linear and the branched one. These results indicate that the alkoxy silane functional group can decrease the filler-filler interaction resulting in smaller silica particle sizes in the compounds.

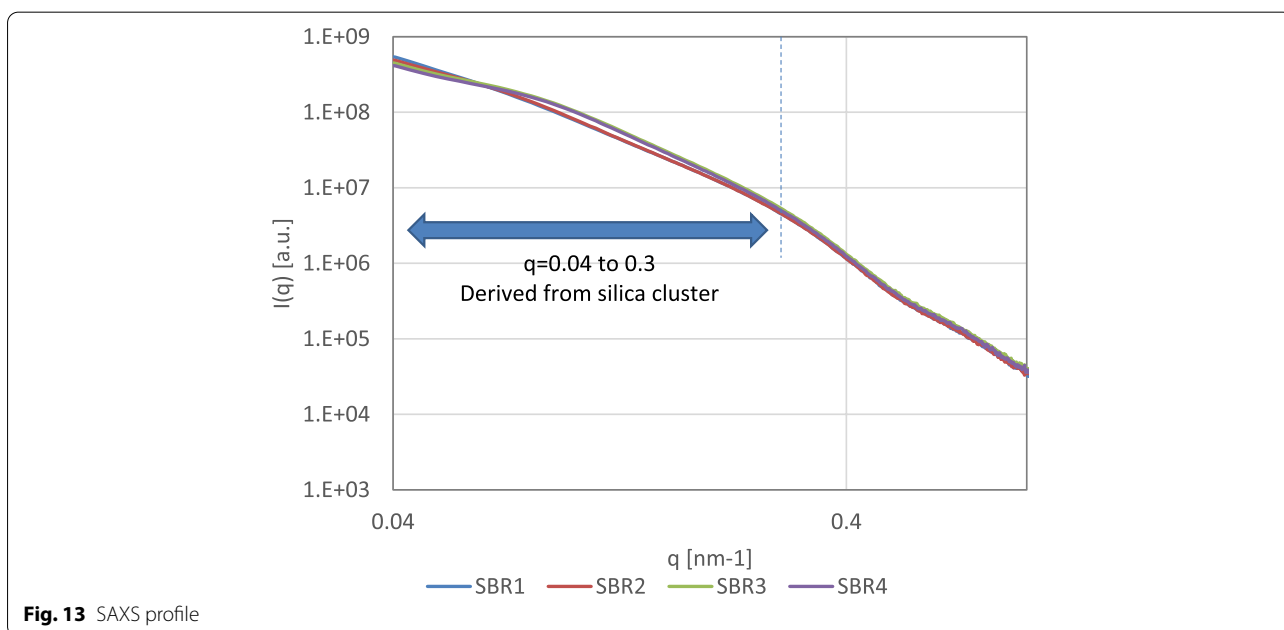
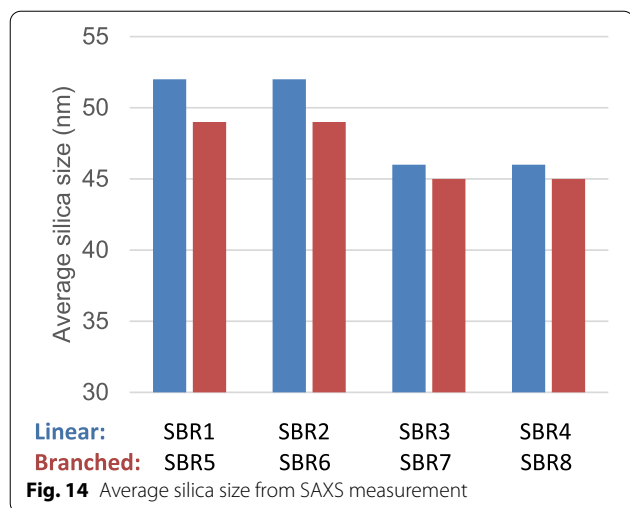


Fig. 13 SAXS profile



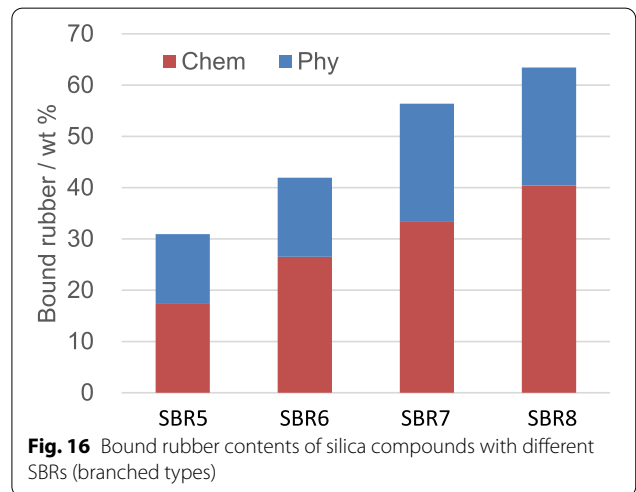
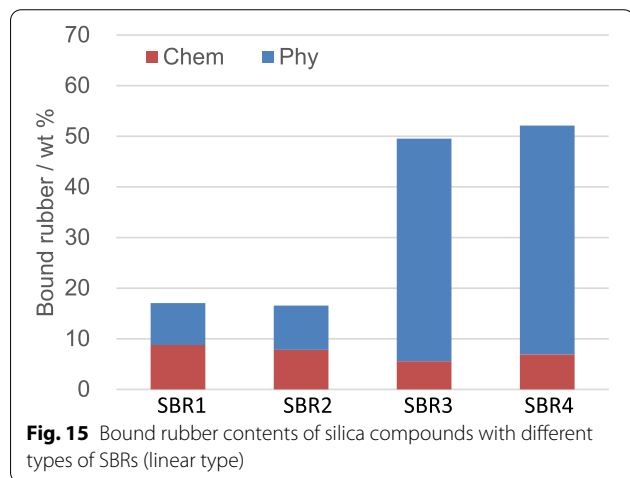
Bound rubber

The amount of chemical bound rubber and physical bound rubber is depicted in Fig. 15.

The amount of chemical bound rubber is almost constant in each SBR type considering the measurement error of $\pm 3\%$. Due to the fact that the alkoxy silane-groups at the end of the polymer chains of SBR 3 and SBR 4 can interact with silica and create a covalent bond, the result did not agree with the expectation. The reason might be that the mixing temperature of 140 °C was not high enough for the expected reaction between the silanol groups and the alkoxy silane-functional group, which leads to the observed constant amount of chemical bound rubber in all SBR compounds. The physical bound rubber content increases in the compounds with SBR 3 and 4. Normally, physical bound rubber includes the rubber which is occluded in silica

particles, named “occluded rubber”. This occluded rubber would increase in compounds having a worse filler dispersion. However, the alkoxy silane functional group in SBR 3 and 4 includes amine, and the hydrogen bonding between amine and silica can be broken in ammonia atmosphere. This is the reason why more physical bound rubber was obtained in SBR 3 and 4.

The bound rubber result of the compounds with branched SBRs is shown in Fig. 16. In this case, the amount of physical bound rubber is almost constant in all SBRs, however, the amount of chemical bound rubber increases in the presence of a higher amount as well as more polar functional groups, such as alkoxy silane group of the modified SBRs. This result differs from the one of the linear SBRs. As mentioned above, the mixing temperature of 140 °C is considered to be not sufficient to start the reaction between the functional group and silica, however, the alkoxy silane-functional group in the branched SBRs is more reactive compared to the one in the linear SBRs, the increase in chemical bound rubber of the alkoxy silane-functionalized SBR compound indicates more filler-polymer interaction by this functional group. The increase of the chemical bound rubber of amine functionalized SBR is due to the acceleration of the silanization reaction of TESPT with the silanol groups. It was found in the model study that the amine group can accelerate the silanization reaction, therefore, the amount of chemical bound rubber of functionalized SBRs is increased. It is estimated that the branched structure itself can also increase the bound rubber as shown in Fig. 17. The molecular weight of the branched SBR is much higher compared to the corresponding linear SBR. Therefore, once the functional group in SBR reacts with silica or TESPT, or TESPT reacts with the SBR chain, more chemical bound rubber is generated in branched SBR compounds.



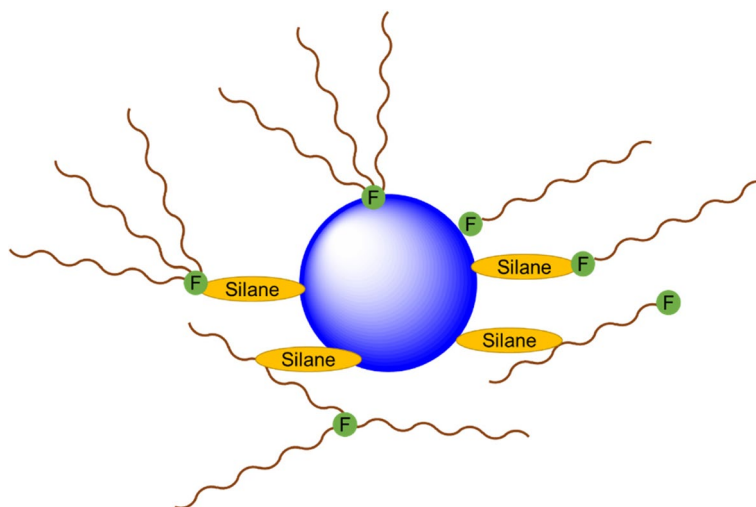


Fig. 17 Branched functionalized SBR and linear functionalized SBR

Table 5 Cure properties

No		1	2	3	4	5	6	7	8
T90	min	28.3	26.0	18.7	15.2	22.0	20.4	18.2	18.5
ML	dNm	1.8	1.7	2.2	2	2.8	2.2	1.9	2.0
MH	dNm	25.1	25.5	19.7	20.7	24.0	22.5	14.3	15.3
MH-ML	dNm	23.3	23.8	17.5	18.6	21.3	20.3	12.3	13.3

Cure behaviors

The cure behaviors are summarized in Table 5. The torque is the indication of the crosslinking density but is consists of contributions from the polymer–polymer, polymer–filler and filler–filler interactions. The gap between the maximum torque (MH) and the minimum tongue (ML) which is an indicator of the crosslink density was smaller in the compound with the functionalized SBRs compared to the non–functionalized SBRs, respectively. Expecting that the polymer–filler interaction is higher in the functionalized SBR compound, this result implies that there is less filler–filler interaction in those compounds with the functionalized SBRs compared to the corresponding non–functionalized SBR compound.

Tensile properties

Tensile properties are depicted in Fig. 18 and Table 6. S200 (the stress at 200% strain) is depicted instead of the stress at 300% elongation because the elongation did not reach 300%. For the linear SBR-based compounds, there is no clear tendency in S200. However, S200 of SBR 6 and SBR 8 is higher than those of SBR 5 and SBR 7, respectively. --This phenomenon is also seen in the

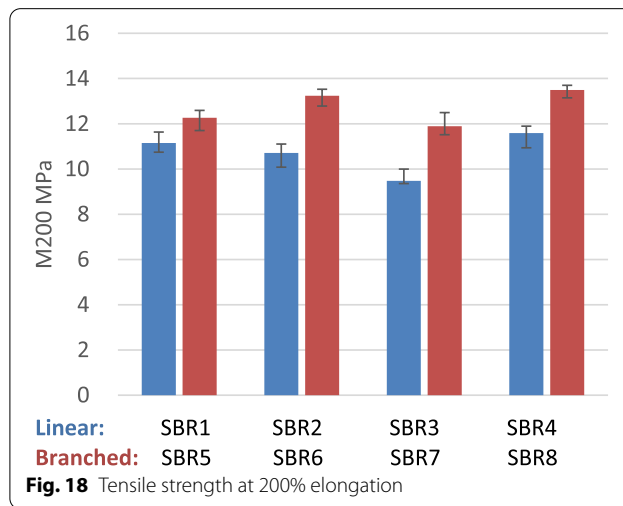
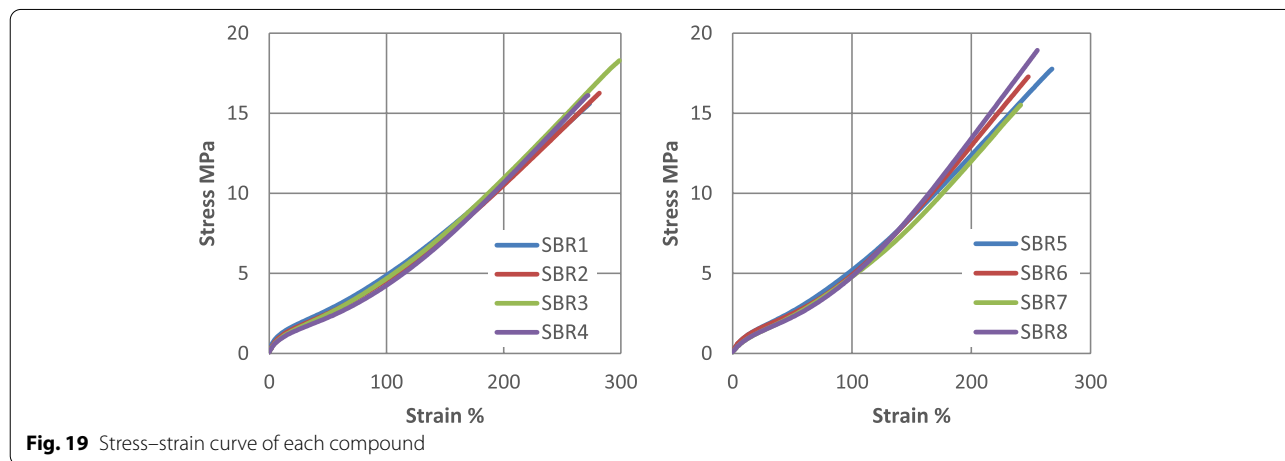


Fig. 18 Tensile strength at 200% elongation

stress–strain curves depicted in Fig. 19. The stress–strain curve of SBR 6 and SBR 8 are slightly higher than SBR 5 and SBR 7, respectively, which indicates the stronger polymer–filler interaction due to the presence of the functional group B in SBR. This tendency is observed only in branched SBRs. The number of the functional group

Table 6 Tensile properties

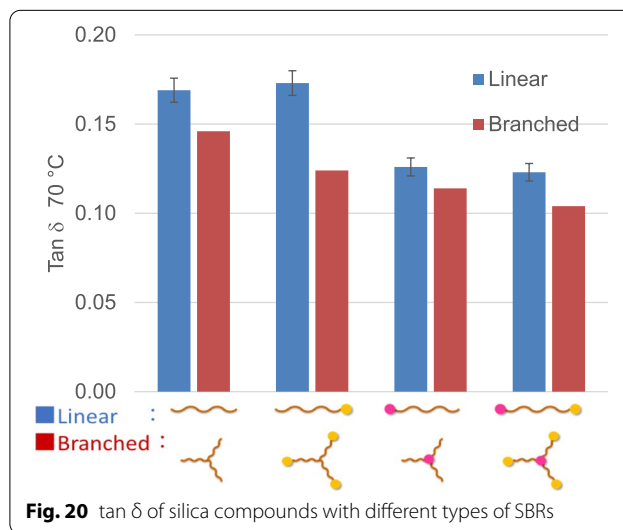
No		1	2	3	4	5	6	7	8
S200	MPa	11.1	10.7	9.5	11.6	12.3	13.2	11.9	13.5
TS	MPa	16.2	15.5	16.4	17.7	16.8	16.5	15.5	18.1
EB	%	276	262	297	272	263	242	241	250



B in one polymer molecule is higher in the branched SBR compared to the linear type. Therefore, the polymer–filler interaction is increased by the presence of the functional group B only in the branched type resulting in higher strain curves and higher S200 values.

Tan δ (indicator of rolling resistance)

It is described in the literature that tan δ between 50 and 70 °C can be used for the indicator of rolling resistance [28]. The tan δ of vulcanized compounds with different types of SBRs is depicted in Fig. 20. In the linear types of SBR, the tan δ of the SBR 1 and SBR 2 compounds is nearly at the same level. This indicates that there is no significant influence of the amine functional group on tan δ. The same tendency can be seen in the result of SBR 3 and 4. But there is a significant decrease of tan δ of the compounds with SBR 3 and 4 compared to those of SBR 1 and 2. This result indicates that the effect of the alkoxy silane functional group is much larger than the amine group. In the branched SBR types, there is a significant difference in the tan δ between amine functionalized SBR 7 and non-functionalized SBR 6. In branched SBR, there is a higher number of amine functional groups in one molecule, therefore, the silanization was accelerated to a higher degree resulting in a reduced tan δ. Comparing the branched SBR and linear SBR, the use of all branched SBRs lead to a lower tan δ. This can be explained by the fact that more bound rubber is formed in branched SBRs.



Conclusions

The influence of the two types of functional groups in SBR on the silica–filled compound was investigated by evaluating the viscoelastic properties, the silica size from SAXS measurements, the bound rubber content, and the mechanical properties. A model reaction was also conducted to investigate the influence of the amine group on the silanization reaction.

1. The model silanization reaction of TESPT with silica in the presence of amine shows that a higher amount of EtOH is released from TESPT compared to the amine free system. This result indicates that the amine could enhance the hydrolysis of TESPT and could accelerate the silanization reaction. From this result it can be expected that the silanization reaction is also accelerated by the presence of an amine functional group at the SBR polymer chain used in silica-filled compounds.
2. The amine functionalized SBR and the alkoxy silane functionalized SBR show less Payne effect of the compounds which indicates that both functional groups can decrease the filler-filler interaction. In both end-functionalized SBRs, the Payne effect value is higher compared to the alkoxy silane-functionalized SBR. This is based on the higher filler-polymer interaction in both-end-functionalized SBR compounds. Additionally, this interaction increases the storage modulus for all strains.
3. More chemical bound rubber was obtained in branched SBRs compared to the corresponding linear SBRs. A branched polymer chain has a higher molecular weight compared to the linear type. Therefore, when one branched polymer chain reacts with silica or creates a silica-silane-polymer bond, more bound rubber can be obtained for the branched than for the linear type.
4. S200 of each SBR compound is comparable in the linear types whereas a significant increase of S200 is observed in SBR with an amine functional group for the branched type SBR compounds. This indicates that the number of the functional groups can influence the polymer-filler interaction.
5. The compound of the SBR with the alkoxy-silane functional group shows lower $\tan \delta$ compared to the non-functionalized SBR and the amine functionalized SBR compounds. The influence of the type of functionalization of the SBR on $\tan \delta$ at 70 °C was more significant in branched SBRs than in linear SBRs, due to the before-mentioned effect of the functional group on silanization, the number of the functional group and bound rubber.

Acknowledgements

The authors gratefully acknowledge financial and materials support from Asahi Kasei Corporation (Tokyo, Japan). Part of the SAXS experiments were performed at the BL03XU of SPring-8 with the approval of the Japan Synchrotron Radiation Research Institute (Proposal No. 2017A7201, and 2017B7251).

Authors' contributions

CY carried out the compounding studies, designed the polymer structure and drafted the manuscript. AY carried out the polymerization. TM carried out the SAXS measurement and the analysis. AB conceived of the study, participated in its design and coordination, and reviewed and edited the manuscript. All authors read and approved the final manuscript.

Funding

This work was financially supported by Asahi Kasei Corporation (Tokyo, Japan).

Availability of data and materials

The data presented in this study are available on request from the corresponding author.

Declarations

Ethics approval and consent to participate

Not applicable.

Consent for publication

Not applicable.

Competing interests

The authors declare that they have no competing interests.

Author details

¹Elastomer Technology and Engineering, University of Twente, Enschede (NL), P.O. Box 217, 7500AE Enschede, the Netherlands. ²Asahi Kasei Corporation, 1-1-2 Yurakucho, Chiyoda-ku, Tokyo 100-0006, Japan.

Received: 19 July 2022 Accepted: 7 October 2022

Published online: 24 October 2022

References

1. D.J. Schuring, S. Futamura, Rolling Loss of Pneumatic Highway Tires in the Eighties. *Rubber Chem. Technol.* **63**(3), 315–367 (1990)
2. R. Rauline, Rubber compound and tires based on such a compound, EP 0501227 A1 (1992)
3. D.C. Edwards, K. Sato, Interaction of Silica with Functionalized SBR. *Rubber Chem. Technol.* **53**(1), 66–79 (1980)
4. M. Rössle, S. Thiele, D. Thielemann, Use of specific aminosilyl monomers in the manufacture of rubber, EP 3434699 A1 (2019)
5. T. Sakurai, S. Nishimura, T. Iizuka, Method of production of conjugated diene rubber, EP 3315535 A1 (2018)
6. K. Morishita, M. Inoue, D. Yoshii, Y. Amano, Method for producing modified conjugated diene polymer, modified conjugated diene polymer, polymer composition, crosslinked body, tire and compound, EP 3476866 A1 (2019)
7. H. W. Lee, W. H. Kim, S. D. Lee, Modified conjugated diene-based polymer and rubber composition comprising same, EP 3536721 A1 (2019)
8. T. Kawai, Development of Modified Solution SBR for the Reduction of Rolling Resistance of Tire, in *Presented at the Fall 182nd Technical Meeting of Rubber Division, ACS Cincinnati, Ohio.* (2012), p.18. (October 9–11, 2012)
9. L. Xiao et al., Preparation, structure, and properties of solution-polymerized styrene-butadiene rubber with functionalized end-groups and its silica-filled composites. *Polymer* **55**(8), 1964–1976 (2014)
10. M. Hassanabadi et al., Synthesis and characterization of end-functionalized solution polymerized styrene-butadiene rubber and study the impact of silica dispersion improvement on the wear behavior of the composite. *Polym. Testing* **85**, 106431 (2020)
11. A.R. Payne, R.E. Whittaker, Low Strain Dynamic Properties of Filled Rubbers. *Rubber Chem. Technol.* **44**(2), 440–478 (1971)
12. T. Koga et al., New Insight into Hierarchical Structures of Carbon Black Dispersed in Polymer Matrices: A Combined Small-Angle Scattering Study. *Macromolecules* **41**(2), 453–464 (2008)
13. S. Mihara et al., Observation of Silica-filled Rubber Using Simultaneous Measurement of Time-resolved Ultra-small Angle X-ray Scattering and Viscoelastic Properties. *Spring-8/SACLA Res. Rep.* **5**(1), 92–96 (2017)
14. S. Mihara et al., Structural Analysis of Silica-filled Rubber Under Cyclic Deformation Using Time-resolved Ultra-small Angle X-ray Scattering. *SPring-8Sect. B Ind. Appl. Rep.* **6**, 297 (2018)
15. M. Kyo, S. Sekikawa, Modified conjugated diene polymer and rubber composition thereof, and tire, JP 2018028047A (2018)
16. S. Wolff, Chemical Aspects of Rubber Reinforcement by Fillers. *Rubber Chem. Technol.* **69**(3), 325–346 (1996)

17. S. Mihara, *Reactive processing of silica-reinforced tire rubber : new insight into the time- and temperature-dependence of silica rubber interaction* (2009)
18. K.-J. Kim, J. VanderKooi, Moisture Effects on TESPD-Silica/CB/SBR Compounds. *Rubber Chem. Technol.* **78**(1), 84–104 (2005)
19. J. Liu et al., Insights into the Silanization Processes of Silica with and without Acid-Base Additives via TG-FTIR and Kinetic Simulation. *Ind. Eng. Chem. Res.* **56**(18), 5164–5173 (2017)
20. A. Hunsche et al., Investigations concerning the reaction silica/organosilane and organosilane/polymer. Part 1: Reaction mechanism and reaction model for silica / organosilane. *KGK-Kautsch. Gummi Kunstst.* **50**(12), 881–889 (1997)
21. A.R. Payne, The dynamic properties of carbon black-loaded natural rubber vulcanizates. Part I. *J. Appl. Polym. Sci.* **6**(19), 57–63 (1962)
22. S.S. Sarkawi, W.K. Dierkes, J.W.M. Noordermeer, Morphology of silica-reinforced natural rubber: the effect of silane coupling agent. *Rubber Chem. Technol.* **88**(3), 359–372 (2015)
23. J. Jin et al., The origin of marching modulus of silica-filled tire tread compounds. *Rubber Chem. Technol.* **93**(2), 378–394 (2019)
24. F. Grunert, *Analytical method development to predict the in-rubber dispersibility of silica* (The university of Twente, Enschede, 2018)
25. M. Takenaka, Analysis of structures of rubber-filler systems with combined scattering methods. *Polym. J.* **45**(1), 10–19 (2013)
26. ASTM Standard D3053 (2020), Standard Terminology Relating to Carbon Black, ASTM International: West Conshohocken, PA, 2020, <https://doi.org/10.1520/D3053-20A>, <https://www.astm.org/>.
27. M. Takenaka, Analyses of Hierarchical Structures of Soft Materials by Using Combined Scattering Methods. *Nippon Gomu Kyokaishi* **84**(1), 7–13 (2011)
28. K.H. Nordsiek, 'Integral rubber' concept - an approach to an ideal tire tread rubber. *Kautsch. Gummi Kunstst.* **38**(3), 178–185 (1985)

Publisher's Note

Springer Nature remains neutral with regard to jurisdictional claims in published maps and institutional affiliations.

Submit your manuscript to a SpringerOpen[®] journal and benefit from:

- ▶ Convenient online submission
- ▶ Rigorous peer review
- ▶ Open access: articles freely available online
- ▶ High visibility within the field
- ▶ Retaining the copyright to your article

Submit your next manuscript at ▶ [springeropen.com](https://www.springeropen.com)
